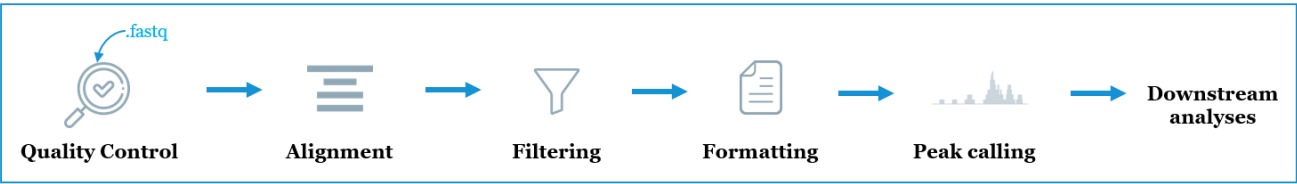


Data (pre)processing



Downstream analyses

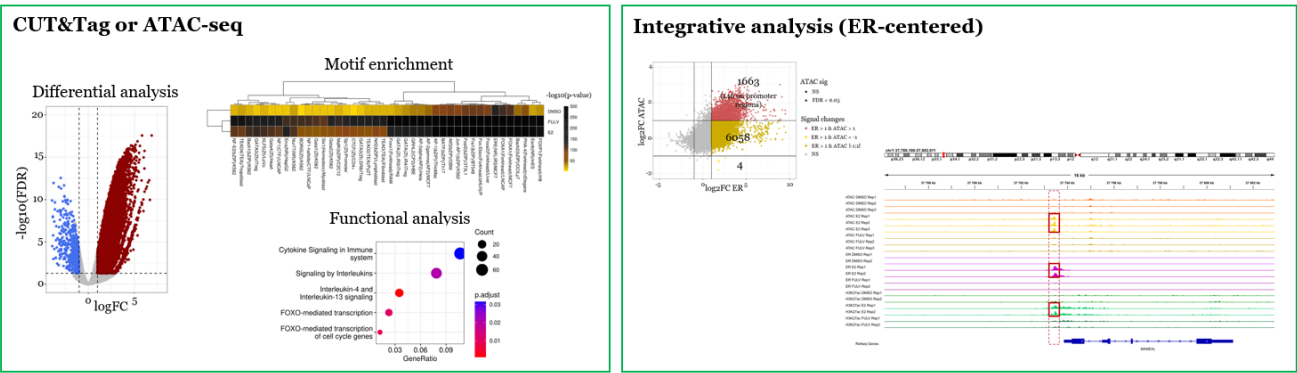


Figure S1. Overview of data processing workflow. Fastq files are first pre-processed for peak calling before downstream analyses. Briefly, a quality control is performed to ensure samples meet quality criteria for further analyses and low-quality reads are filtered out if required. Then, reads are mapped to the human genome hg38 and low-quality mapping reads are removed. In addition, duplicates and blacklisted regions are removed before the peak calling step. Finally, peaks are called using MACS3 and tracks files are generated to visualize signals. The list of peaks is then used to generate a count matrix which is used for downstream analyses. In that regard, similar downstream analyses were performed for CUT&Tag (ER, H3K27ac) and ATAC-seq datasets including a differential analysis comparing treatments and control, a functional analysis based on differential sites and a DNA motif enrichment. Data were then integrated to identify ER binding sites with dysregulation of chromatin accessibility and/or H3K27ac signals.

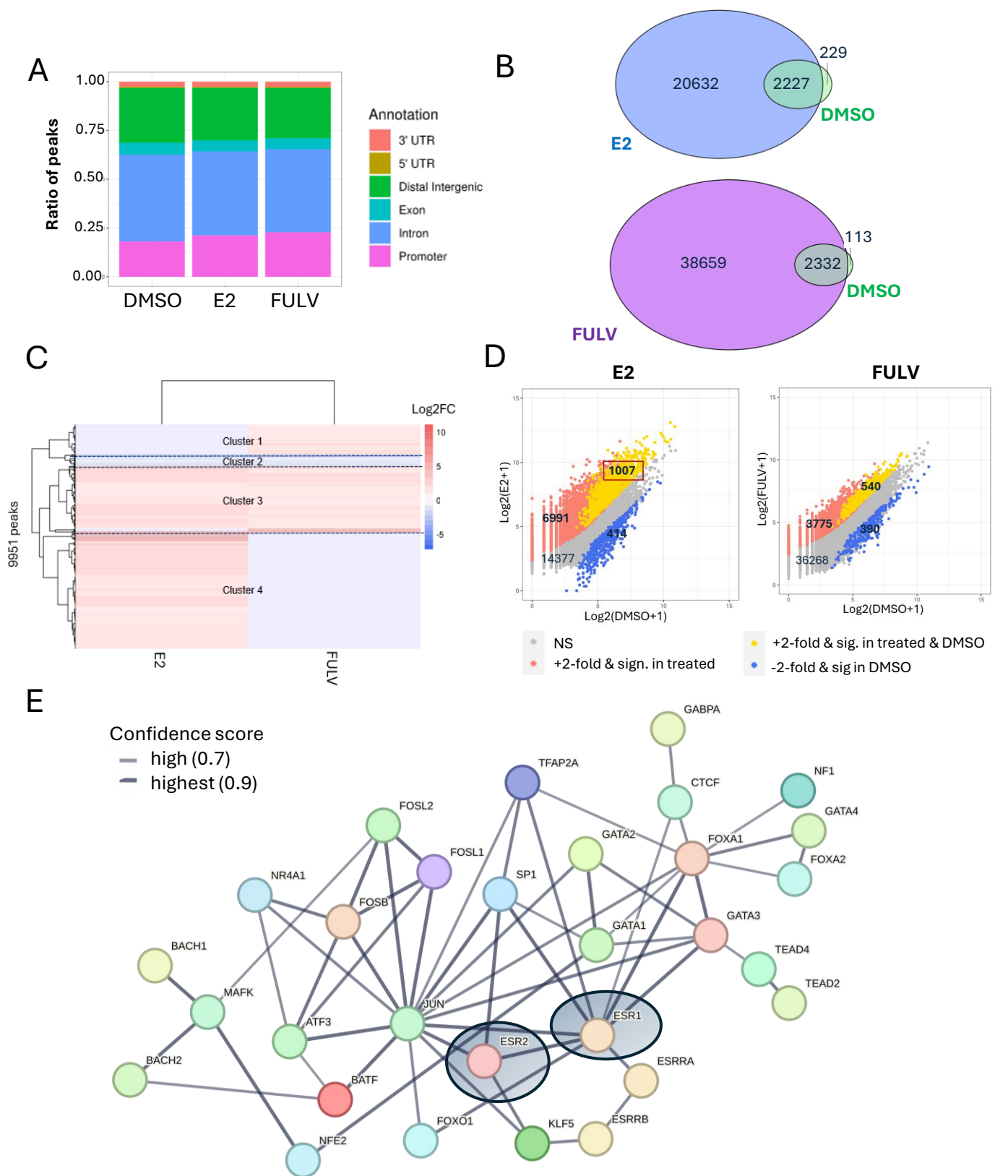
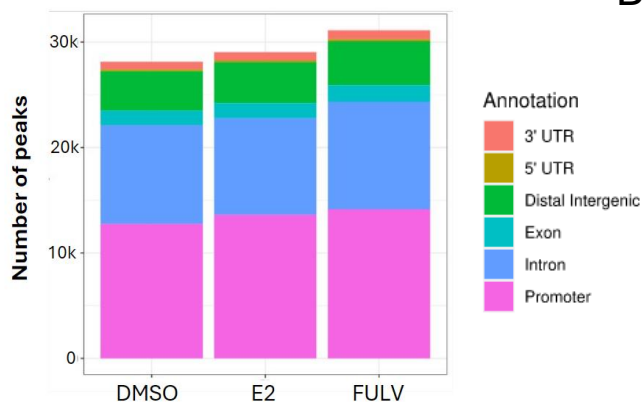
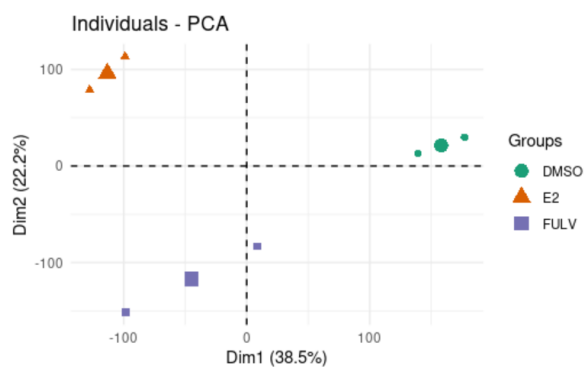


Figure S2. Characterization of ER binding sites identified upon E2 and FULV treatments. (A) Bar plots show the genomic distribution of ER binding sites across conditions. Less than 25% ER peaks fall inside promoter regions (B) Venn diagrams highlight the dramatic increase of ER binding sites upon treatment and shows the large overlap with pre-existing binding sites in the control DMSO condition. Peaks with at least 1bp in common were considered as overlapping (C) Heatmap shows differential ER Cut&Tag signals at 9951 ER binding sites found to be significantly differentially enriched in at least one treatment condition. Positive log2FC in red for increasing signals and negative log2FC in blue for decreasing signals. Four clusters are identified: cluster 1 contains ER sites specifically enriched upon FULV treatment, cluster 2 contains ER sites depleted in both treatment conditions, cluster 3 contains ER sites enriched in both treatment conditions and cluster 4 contains ER sites specifically enriched upon E2 treatment (D) Scatterplots shows the normalized ER Cut&Tag signals in the DMSO control and the annotated treatment condition at ER peaks shown in B. In yellow: peaks were called in both the treated and control conditions, and a minimum 2-fold signal increase is observed upon treatment; in red: peaks were only called upon treatment, and a minimum 2-fold signal increase is observed upon treatment; in blue: peaks were called in the control and/or the treated condition, and a minimum 2-fold signal increase is observed in the control; in grey: no significant changes upon treatment (E) Protein-protein interaction network of transcription factors inferred from DNA motifs enriched with at least $p < 1e-100$ in DMSO and/or E2 and/or FULV displayed in Figure 2D. The ERE motif directly linked to ER resulted in ESR1 and ESR2 transcription factors highlighted in the network.

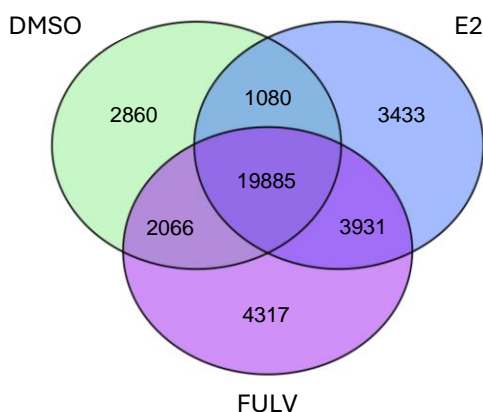
A



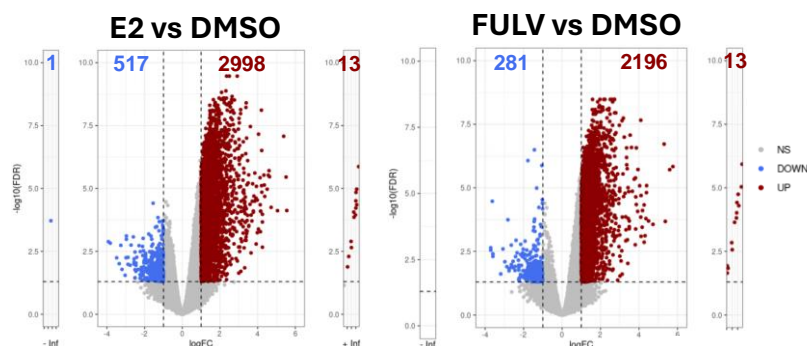
B



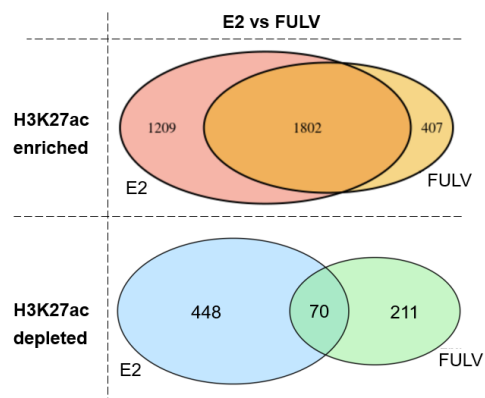
C



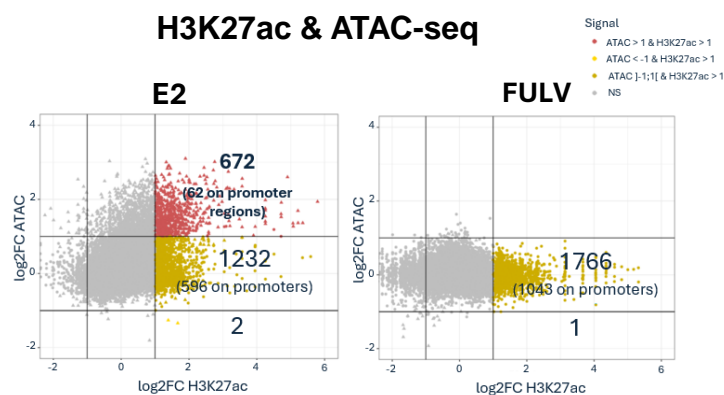
D



E



F



G

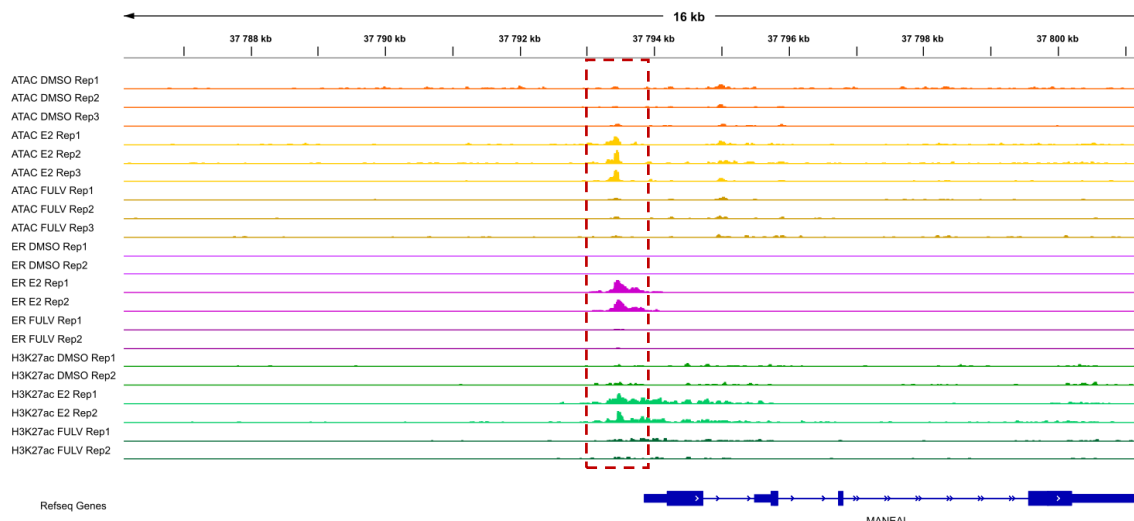


Figure S3. Genome-wide H3K27ac signal changes upon FULV and E2 treatments. (A) Bar plots show the number and genomic distribution of H3K27ac binding sites across conditions (B) Principal Component Analysis plot based on the fragments counted in H3K27ac peaks called across conditions. Experimental conditions are well separated from each other and replicates remain grouped together based on genome-wide H3K27ac signals. A larger symbol represents the centroid of the cluster for each condition (C) Venn diagram shows the overlap of H3K27ac peaks coordinates across experimental condition. Despite a large overlap with pre-existing sites in the control DMSO condition, a large number of sites are specific for each condition (D) Volcano plots show differential H3K27ac signals compared to the DMSO control condition. Both treatments induce robust H3K27ac changes genome-wide. In blue, H3K27ac signal is significantly decreased at least 2-fold upon treatment ($FDR < 0.05$) and in red, H3K27ac signal is significantly increased at least 2-fold upon treatment ($FDR < 0.05$). Non significant changes are displayed in grey. $-\text{Inf}$ and $+\text{Inf}$ panels contain peaks for which no counts were found in one of the condition: in $-\text{inf}$ no count was found in the treated condition for the specific peak and, in $+\text{inf}$ no count was found in the control condition. (E) Venn diagrams show the overlap between H3K27ac enriched or depleted regions detected upon E2 and FULV treatments. Most H3K27ac enriched regions are common to both E2 and FULV conditions whereas depleted H3K27ac regions appear treatment specific (F) Scatterplots show H3K27ac Cut&Tag and ATAC-seq signal changes at ER binding sites upon E2 or FULV treatment. In red, a minimum 2-fold increase in both ATAC-seq and H3K27ac Cut&Tag signals is observed upon treatment; in light yellow, a minimum 2-fold increase in H3K27ac Cut&Tag signal concomitant with a minimum 2-fold decrease in ATAC-seq signal; in dark gold, a minimum 2-fold increase in H3K27ac Cut&Tag signal concomitant with mild to no change in ATAC-seq signal; The shape of the dots reflects the significance of ATAC-seq signal changes with a triangle showing significant changes ($FDR < 0.05$) (G) Representative example near the *MANEAL* locus showing increased ER Cut&Tag signals upon E2 treatment in the MCF7 breast cancer cell line with concomitant increases in ATAC-seq and H3K27ac Cut&Tag signals. No changes were detected upon FULV treatment in this region.